Bonding and strength of solid nitrogen in the cubic gauche (cg-N) structure

Xing-Qiu Chen,[1,*] C. L. Fu,[1] and R. Podloucky[2]

[1]*Materials Science and Technology Division, Oak Ridge National Laboratory, Oak Ridge, Tennessee, 37831-6114, USA*
[2]*Institut für Physikalische Chemie, Universität Wien, Sensengasse 8/7, A-1090, Vienna, Austria*

Recently, the unusual high-pressure cubic gauche structure of solid nitrogen (cg-N) was experimentally synthesized. Our first-principles calculations reveal that cg-N represents a new class of covalent solids in which the atoms are threefold coordinated, yet the structure is stabilized by the presence of near-tetrahedral sp^3-hybridized electronic states. This bonding scheme results in a strong covalency, exceptional mechanical properties, and the stabilization of cg-N as a high-energy-capacity material. The cg-N is an insulator with a wide gap that is nearly constant over a wide pressure range. The mechanical failure mode in cg-N is dominated by the shear type, and the calculated (110) $\langle 1\bar{1}0 \rangle$ shear strength of 41.3 GPa (at which the lattice becomes unstable) sets an upper bound for its ideal strength. This shear-induced structural instability is associated with the structural transformation from the cg-N structure to the monoclinic structure.

I. INTRODUCTION

In recent years, the nature of solid nitrogen under pressure has attracted great interest due to its fundamental and technological importance.[1–12] Specifically, considerable effort[1–6] has been devoted to synthesizing polymeric network forms of nitrogen, particularly the single-bonded threefold-coordinated polymeric nitrogen, due to their promising potential as high-energy-density materials.[5,13] It was proposed theoretically that nitrogen should transform from its ambient diatomic form to a single-bonded crystalline structure at high pressures.[7–9] This single-bonded polymeric nitrogen structure was identified to have the cubic gauche structure by Mailhiot *et al.*[9] Recently, at high pressures (above 110 GPa) and high temperatures (2000 K), Eremets *et al.*[2] synthesized the long-sought single-bonded cubic gauche structure of nitrogen (cg-N). This new form was found to be stable down to at least 40 GPa.

The cubic gauche structure has never been observed previously for any other element, rendering cg-N a very special material. In this paper, through first-principles electronic structure calculations, we demonstrate that cg-N is a wide-band-gap insulator with a nearly constant gap over a wide pressure range. Furthermore, cg-N is found to have high tensile and shear strength at zero pressure. These intriguing properties of cg-N can be attributed to its unconventional bonding scheme. Although the nitrogen atoms in cg-N are threefold coordinated, we find that the electronic states in cg-N are actually characterized by the tetrahedral-like sp^3 hybrids (i.e., a hybridization scheme similar to that of tetrahedral-bonded diamond[14]). Since a nitrogen atom has five valence electrons, the three single-bonded covalent bonds that connect each nitrogen atom to its three nearest neighbors in cg-N are, in fact, stabilized by the presence of a lone-pair nonbonding orbital which accommodates a pair of electrons. This bonding scheme has an analogy to the strong covalency of the sp^2 state in graphite (as manifested in the short bond length of cg-N) but with the bond angle similar to that of the sp^3 orbitals in diamond.

In Sec. II, the theoretical model and computational method are briefly described. The calculated results for structural parameters, electronic structure, band gaps, elastic constants, and ideal strength (both tensile and shear) are presented in Sec. III. In the discussion of electronic structure, emphasis is placed on its unique bonding scheme based on the tetrahedral-like sp^3 hybrids. The band gaps and their pressure dependence are compared among cg-N, diamond, and Si. The elastic constants and ideal strength are compared among cg-N, diamond, and c-BN. A summary is given in the last section.

II. COMPUTATIONAL METHOD

Our first-principles calculations were performed using the Vienna *ab initio* simulation package[15] (VASP) with the ion-electron interaction described by the projector augmented-wave potential. We used both the generalized gradient approximation [GGA (Ref. 16)] and local density approximation [LDA (Ref. 17)] for the exchange-correlation functional. Brillouin-zone integrations were performed using k-mesh $21 \times 21 \times 21$ for special k points according to the Monkhorst-Pack technique. The energy cutoff for the plane-wave expansion of eigenfunctions was set to 400 eV. Optimization of structural parameters was achieved by the minimization of forces and stress tensors.

The three independent elastic constants of cg-N were derived from the total energies as a function of lattice strains. These strain energies were fitted to third-order polynomials from which the elastic constants at the equilibrium structures were calculated.[19] In order to calculate the tensile and shear strength of cg-N, we employed the method described in Refs. 20–22. The lattice vectors were incrementally deformed in the direction of the applied stress. At each step of incremental strain, we allowed the full relaxation of the lattice basis vectors and the strain components orthogonal to the direction of the applied stress.

III. RESULTS AND DISCUSSION

A. Structural properties

Experiments[2] demonstrated that solid cg-N at 115.4 GPa (i.e., the pressure at which the cg-N was synthesized) adopts

TABLE I. The lattice constant a (Å), volume V (Å^3/atom), bulk modulus B (GPa), and the internal parameter x at the $8a$ (x,x,x) sites calculated for cg-N at zero and experimental pressures.

		Calc.	Expt.[a]		Calc.	Calc.[b]
Pressure (GPa)		0	0	115.4	115.4	115.4
a	GGA	3.793	3.752[c]	3.454	3.484	3.494
	LDA	3.747			3.457	
V	GGA	6.825	6.60[c]	5.15	5.288	
	LDA	6.566			5.163	
B	GGA	297	301±0.9			281
	LDA	325				
x	GGA	0.083		0.067	0.072	0.073
	LDA	0.087			0.073	

[a]References 2 and 5.
[b]Reference 12.
[c]The experimental values are obtained by extrapolation of the experimental pressure-volume equation of state to zero pressure (Ref. 5).

the space group $I2_13$ with N atoms at the $8a$ (x,x,x) sites (where $x=0.067$). The cg-N unit cell contains eight nitrogen atoms (four atoms in the primitive cell). In cg-N each nitrogen atom is connected to three neighbors with three single covalent bonds. The calculated structural parameters listed in Table I are consistent with those of recent calculations.[12] At zero pressure, the parameters obtained by the LDA (GGA) are $a=3.747$ (3.793) Å, agreeing very well with the lattice constant of 3.752 Å extrapolated from the experimental pressure-volume states of equations.[5] The bulk modulus B and pressure derivative B are 325 (297) GPa and 4.1 (3.9) by the LDA (GGA), respectively, also in good agreement with the experimental results ($B=301±0.9$ GPa and $B'=4.02$). For the bulk modulus, the LDA value is larger than the GGA value due to the known characteristic that the LDA (GGA) tends to underestimate (overestimate) the equilibrium volume. The positional parameter x decreases slightly with increasing pressure. At 115.4 GPa, x is about 0.070, which is in excellent agreement with the experimental value (0.0672). For pressures above 750 GPa, x is found to be zero, implying that the cg-N structure is reduced to a simple cubic one (Po type).

B. Electronic bonding properties

Figure 1 shows the band structure and density of states (DOS) for cg-N. The occupied states consist of two major groups, separated by an indirect gap of 3.5 eV. The lowest-energy states (more than 9 eV below the top of the valence band) consist of hybridized covalent bonding states, as illustrated by the charge density isosurface shown in Fig. 2(a). Integration over these states shows that there are only three bonds of this type per atom. Note that these trigonal covalent bonds are fundamentally different from the sp^2-bonding scheme that would require a planar bonding with an angle of 120° between orbitals. Instead, as shown in Fig. 2(b), the bond angle in cg-N under pressure is rather close to the value of 109.3° for sp^3 bonds in diamond. The second lowest group of occupied states, ranging from −6 eV to the top of

the valence band, consists of nonbonding states, which relate to a lone-pair orbital. Its nonbonding nature is illustrated by the isosurface shown in Fig. 2(c), which clearly is not localized along neighboring atom bonds. Integration of these nonbonding states yields two electrons per atom.

Although we have described the bonding in terms of the characteristics of two groups of occupied states, the electronic states in cg-N are, in fact, sp^3 hybrids. These hybrids are intrinsically different from the sp^3 states in group-IV and III-V materials (e.g., diamond structure), in which the four covalent bonds connecting each atom to its four neighbors are equivalent. For the sp^3 hybrids of cg-N, there are three covalent bands connecting each nitrogen atom to its three neighbors; the remaining two electrons form a lone-pair orbital, which does not participate in the direct bonding with other atoms. In other words, in order to accommodate five valence electrons of nitrogen in a stable tetrahedral-like
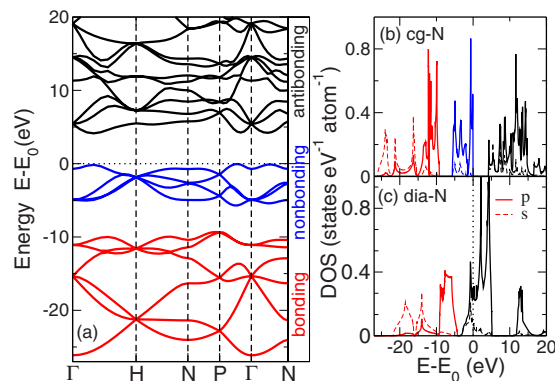

FIG. 1. (Color online) (a) Electronic band structure of cg-N along the high-symmetry direction from LDA calculations; (b) and (c) density of states (DOS in states eV^{-1} atom^{-1}) at zero pressure for cg-N and dia-N (hypothetical diamond phase of nitrogen), respectively. Zero energy (E_0) denotes the Fermi energy of the dia-N phase and the top of the valence band of the cg-N phase. In cg-N, the states with energy lower than E_0 are fully occupied and the antibonding states are unoccupied.
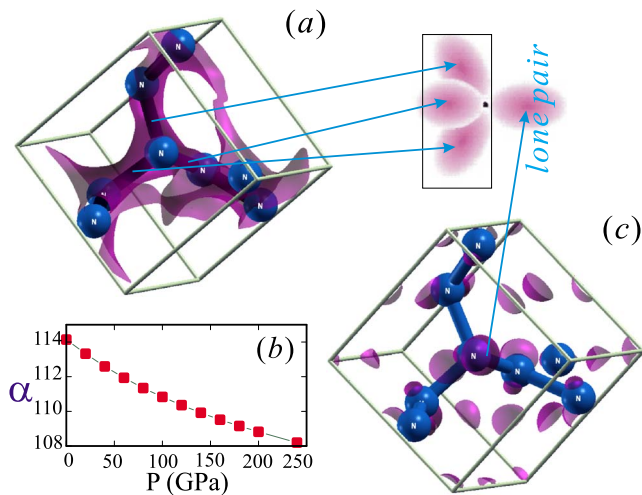
FIG. 2. (Color online) Schematic illustration of sp^3 hybrids in cg-N. (a) Isosurface of constant charge density (at a value of $2.2e/\text{Å}^3$) for the bonding states in the energy range from -30 eV to -9 eV. (b) Pressure dependence of the bond angle α between threefold covalent orbitals. (c) Isosurface of constant charge density (at a value of $1.3e/\text{Å}^3$) for the nonbonding states in the energy range from -6 eV to the top of the valence band.

bonding geometry, the cg-N structure is the necessary and only choice and should have the lowest electronic energy. For comparison, the DOS of solid nitrogen in the diamond structure (dia-N) is also shown in Fig. 1(c). In this bonding geometry, dia-N is metallic and the antibonding states become occupied. As a result, the dia-N phase is much less favorable in energy by about 2.3 eV per atom in comparison to the cg-N phase at zero pressure.

The importance of the sp^3 trigonal covalent bonds for structural stability is further demonstrated in our finding that the cg-N structure is energetically favorable over other solid and molecular phases [α-N (Ref. 9), β-N (Ref. 9), simple cubic (sc) (Ref. 11), and black phosphorus structure (BP) (Ref. 11)] in the pressure range from 31 GPa to 212 GPa. At low pressures, the cg-N transforms into highly stable molecular states with a large release of energy. For example, at zero pressure, the energy difference between single-bonded cg-N and triple-bonded N_2 is calculated to be 4.32 eV/atom. Due to these unique properties, cg-N has been suggested as a promising high-energy-capacity material.[5,13]

C. Band gap and its pressure dependence

The cg-N phase is insulating, as seen from the DOS profile shown in Fig. 1. It is well known that in many cases the gap sizes are not correctly given by density functional theory (DFT) within the LDA or GGA approach. Therefore, additional calculations were made using a hybrid functional approach involving a screened Hartree-Fock exchange ansatz (HSE) as implemented in VASP. This approach was proved to correctly predict band gap of a number of insulators and semiconductors.[18] For instance, for diamond, the calculated direct gap ($\Gamma'_{25} \rightarrow \Gamma_{15}$) of 6.74 eV is in reasonable agreement with the experimental value of 7.3 eV.[23] For cg-N, the LDA
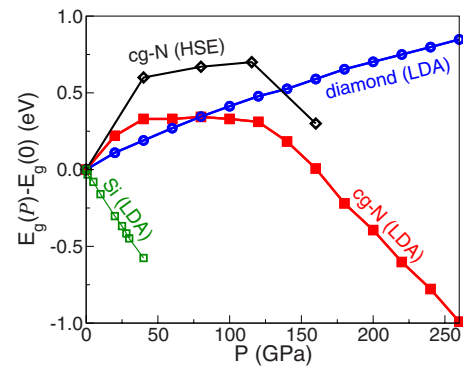

FIG. 3. (Color online) Relative change of band gap, $E_g(P) - E_g(P=0)$, as a function of pressure for diamond, Si and cg-N. At $P=0$, the gaps from DFT-LDA calculations are 4.3 eV for cg-N, 4.2 eV for diamond, and 0.6 eV for Si; the result from the HSE calculation is 7.6 eV for cg-N.

(GGA) predicts a small band gap of 4.3 (4.2) eV (in agreement with previous DFT calculations[11,12]), while the HSE-calculated gap of 7.6 eV agrees well with the value of 8.1 eV derived from a quantum Monte Carlo calculation.[10] All these values refer to zero pressure. This wide band gap is supported by the experimental observation of a colorless transparent cg-N phase.[2]

We have studied the pressure dependence of gap size up to a pressure of 250 GPa. As shown in Fig. 3, the gap of cg-N has a very unusual pressure dependence behavior: the gap increases with increasing pressure up to 40 GPa and remains rather constant between 40 GPa and 130 GPa before decreasing rapidly at higher pressures. The gap calculated from both the LDA (or GGA) and HSE shows a similar pressure dependence, in terms of the range of constant gap and the reduction of the gap size. Analysis of the electronic structure shows that the pressure dependence of gap size is closely related to the band width of nonbonding states (cf. Fig. 4). The bandwidth of nonbonding states is relatively insensitive to pressure below 40 GPa. In this pressure range the broadening of the whole DOS thus results in an increase of the band gap. However, for pressure from 40 to 120 GPa, the broadening of the nonbonding states cancels with the effect of the antibonding interaction in lifting up the conduction band edge, resulting in a constant gap. However, for pressures above 120 GPa, the rate of the broadening of nonbonding states increases more rapidly with increasing pressure, since the lattice is so compressed that even the nonbonding states are strongly affected, leading to a decrease of band gap as pressure increases. For comparison, LDA calculations for the gap of diamond are also shown in Fig. 3, revealing a linear increase of the gap size as a function of pressure, in accordance with experimental and theoretical results.[23,24] Also shown in Fig. 3 is the LDA-predicted gap for Si, which decreases with increasing pressure, becoming metallic at 40 GPa.

D. Elastic constants and ideal strength

The calculated elastic constants of cg-N, listed in Table II, clearly show that cg-N is elastically stable at zero pressure.
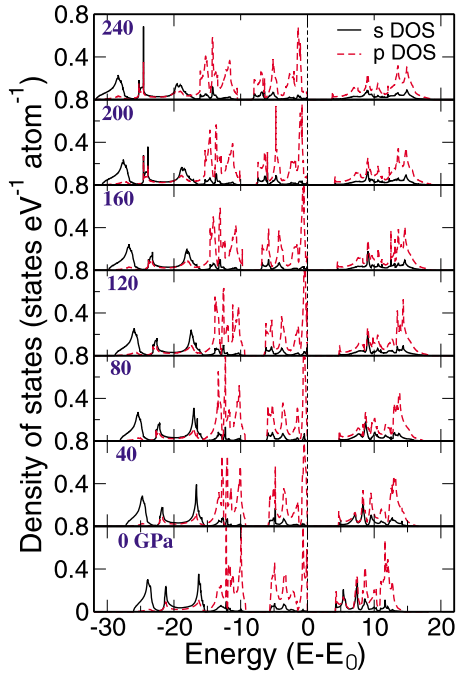
FIG. 4. (Color online) Pressure-dependent electronic densities of states of cg-N from LDA calculations. Zero energy (E_0) denotes the top of the valence band of the cg-N phase. In cg-N, the states with energy lower than E_0 are fully occupied and the antibonding states are unoccupied.

The LDA-calculated elastic constants are slightly higher than those calculated by the GGA mainly due to the difference in the calculated equilibrium volume between the LDA and GGA. The calculated bulk modulus ($B \approx 300$ GPa) agrees well with the experimental value (extrapolated to zero pressure).[2] Our calculated elastic constants (C_{11}, C_{12}, and C_{44}) by the GGA are in reasonable agreement with a previous calculation by Yu *et al.*[12] Based on the Hill-approximation scheme, cg-N is found to have considerably high shear modulus ($G \approx 250$ GPa) and Young's modulus ($E \approx 600$ GPa). Nevertheless, despite the strong covalence in cg-N, the bulk and shear moduli of cg-N are still significantly lower than those of diamond (cf. Table II), since there are only three covalent bonds for each atom in cg-N instead of four for each atom in diamond.
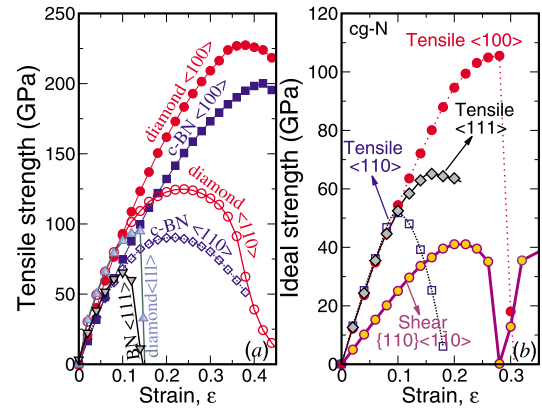

FIG. 5. (Color online) The calculated ideal tensile strength along $\langle 100 \rangle$, $\langle 111 \rangle$, and $\langle 110 \rangle$ directions for (a) diamond and *c*-BN and (b) cg-N. In (b) the calculated stress-strain curve for the (110) $\langle 1\bar{1}0 \rangle$ shear is also shown for cg-N.

For many of the high-strength covalent solids, it is known that the strength and elastic modulus are not necessarily linearly correlated.[25,26] In the absence of defects, the strength is limited by the stress at which the lattice becomes unstable. Thus, we next discuss the ideal strength (both tensile and shear) of cg-N.

The calculations for the ideal strength were carried out using the LDA scheme. As discussed above, cg-N exhibits threefold covalent bonds together with a localized lone-pair nonbonding orbital in the sp^3-bonding scheme. Thus, it is interesting to compare the ideal strength of cg-N with that of the fourfold covalent diamond and *c*-BN (diamondlike zinc-blend structure). In Fig. 5(a) we present the stress-strain relation in the $\langle 100 \rangle$, $\langle 110 \rangle$, and $\langle 111 \rangle$ directions for diamond and c-BN. Our calculated results for the tensile strength of diamond are 227.3, 124.5, and 94.5 GPa in $\langle 100 \rangle$, $\langle 110 \rangle$, and $\langle 111 \rangle$ directions, respectively. The corresponding values for *c*-BN are 199.3, 90.4, and 64.8 GPa. These results are in excellent agreement with those of previous calculations.[27–29] Since it has been shown that the (111) $\langle 11\bar{2} \rangle$ shear strength is higher than the $\langle 111 \rangle$ tensile strength for both diamond and c-BN,[27,29] the failure mode in diamond and c-BN is dominated by the tensile type and the $\langle 111 \rangle$ direction is the weakest.

TABLE II. The calculated elastic constants (C_{ij}), bulk modulus (B), Young's modulus (E), and shear modulus (G) of cg-N and diamond at zero pressure from both LDA and GGA calculations (in units of GPa). For comparison, the experimental data (Refs. 2 and 30) are also listed.

	C_{11}	C_{12}	C_{44}	B	E	G
Cg-N (GGA)	558	160	280	297	573	244
Cg-N (LDA)	579	174	318	309	618	265
Cg-N (expt)[a]				301 ± 0.9		
Diamond (GGA)	1067	132	571	444	1132	527
Diamond (LDA)	1112	147	601	469	1186	550
Diamond (expt)[b]	1079	124	578	443	1144	538

[a]Reference 2.
[b]Reference 30.

The stress-strain curves for cg-N are presented in Fig. 5(b). The magnitudes for the tensile strength in the $\langle 100 \rangle$, $\langle 110 \rangle$, and $\langle 111 \rangle$ directions are predicted to be 105.4, 51.6, and 65.2 GPa, respectively. In all directions, the ideal tensile strength is significantly lower than that of diamond. The weakest tensile strength direction for cg-N is found to be $\langle 110 \rangle$, which is consistent with the fact that the most close-packed plane in the cg-N structure is the (110) plane.

For cg-N, we have also calculated the ideal shear strength for the $\langle 1\bar{1}0 \rangle$ shear on the (110) plane. The shear strength in cg-N is found to be much lower than the tensile strength by as much as 20% [cf. Fig. 5(b)]. In other words, the failure mode in cg-N is dominated by the shear type, which is obviously different from that in diamond and c-BN. For cg-N, the calculated (110) $\langle 1\bar{1}0 \rangle$ shear strength, 41.3 GPa, basically sets the upper bound on its ideal strength at zero pressure.

As mentioned already, the ideal strength is determined by the stress at which the crystal becomes unstable (and typically at a strain beyond the elastic limit). For the case of cg-N, this structural instability is driven by the structural transformation from the orthorhombic to the monoclinic structure as the strain increases.

As shown in Fig. 5(b), for the (110) $\langle 1\bar{1}0 \rangle$ shear, the peak shear stress occurs at a strain of 0.28 and then the strain energy decreases abruptly as the strain further increases [Fig. 6(a)]. The discontinuity in the strain energy suggests that a structural phase transformation occurs at a strain of 0.3. The transformed phase (at a strain of 0.3) has the monoclinic structure with lattice parameters of $a = 7.868$ Å, $b = 3.747$ Å, $c = 12.211$ Å, and $\beta = 162.87°$. We have analyzed the N-N bond length as a function of the strain. As shown in Fig. 6(b), at zero strain, there is only one type of the N-N bond in the cg-N structure; at finite strains, the N-N bond is split into four different types (labeled as $d1$, $d2$, $d3$, and $d4$). Since the occurrence of the structural instability is accompanied by the discontinuity in the bond lengths as a function of strain (cf. Fig. 6), the structural transformation is clearly driven by the release of strain energy by rearranging nitrogen atoms in the strained lattice. We note that, as the strain increases beyond 0.3, the longest N-N bond length is the $d3$ type. Thus, at larger strains, the strained lattice can be viewed as a structure consisting of zigzag chain blocks of nitrogen atoms interconnected by the $d3$-type bonds [cf. Fig. 6(b)]. This type of structural geometry seems to imply that, at even larger stains, the deformed cg-N structure might become the chain-layer solid phase, as found in experiment.[5]

IV. SUMMARY

Our first-principles calculations reveal that cg-N represents a new class of covalent solid in which the atoms are threefold coordinated, yet the structure is stabilized by the
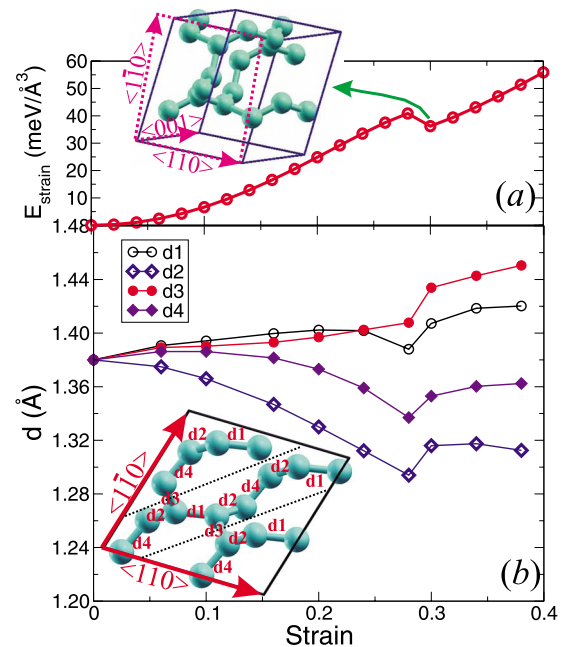

FIG. 6. (Color online) (a) Calculated strain energy as a function of strain for cg-N under the (110) $\langle 1\bar{1}0 \rangle$ shear. Inset: schematic illustration of the strained lattice at a strain of 0.3; the unstrained cell is outlined by the dashed lines. (b) Calculated N-N bond lengths (denoted by $d1$, $d2$, $d3$, and $d4$) as a function of strain for cg-N under the (110) $\langle 1\bar{1}0 \rangle$ shear. Inset: the side view of the strained lattice with the $\langle 001 \rangle$ direction normal to the plane.

presence of near-tetrahedral sp^3-hybridized electronic states. For the sp^3 hybrids of cg-N, there are three covalent bands connecting each nitrogen atom to its three neighbors; the remaining two electrons form a lone-pair orbital, which does not participate in the direct bonding with other atoms. The nonbonding state plays an important role in determining its unique constant-gap behavior under pressure. The mechanical failure mode in cg-N is found to be shear in nature. The calculated (110) $\langle 1\bar{1}0 \rangle$ shear strength of 41.3 GPa (at which the lattice becomes unstable) basically sets an upper bound for its ideal strength. The shear-induced mechanical instability of cg-N is found to be associated with the phase transition into the monoclinic structure.

ACKNOWLEDGMENTS

*chenx@ornl.gov

[1] M. I. Eremets, R. J. Hemley, H. K. Mao, and E. Gregoryanz, Nature (London) **411**, 170 (2001).

[2] M. I. Eremets, A. G. Gavriliuk, I. A. Trojan, D. A. Dzivenko, and R. Boehler, Nat. Mater. **3**, 558 (2004).

[3] W. D. Mattson, D. Sanchez-Portal, S. Chiesa, and R. M. Martin, Phys. Rev. Lett. **93**, 125501 (2004).

[4] A. F. Goncharov, E. Gregoryanz, H.-K. Mao, Z. X. Liu, and R. J. Hemley, Phys. Rev. Lett. **85**, 1262 (2000).

[5] M. I. Eremets, A. G. Gavriliuk, N. R. Serebryanaya, I. A. Trojan, D. A. Dzivenko, R. Boehler, H. K. Mao, and R. J. Hemley, J. Chem. Phys. **121**, 11296 (2004).

[6] E. Gregoryanz, A. F. Goncharov, R. J. Hemley, and H.-K. Mao, Phys. Rev. B **64**, 052103 (2001).

[7] A. K. McMahan and R. LeSar, Phys. Rev. Lett. **54**, 1929 (1985).

[8] R. M. Martin and R. J. Needs, Phys. Rev. B **34**, 5082 (1986).

[9] C. Mailhiot, L. H. Yang, and A. K. McMahan, Phys. Rev. B **46**, 14419 (1992).

[10] L. Mitas and R. M. Martin, Phys. Rev. Lett. **72**, 2438 (1994).

[11] M. M. G. Alemany and J. L. Martins, Phys. Rev. B **68**, 024110 (2003).

[12] H. L. Yu, G. W. Yang, X. H. Yan, Y. Xiao, Y. L. Mao, Y. R. Yang, and M. X. Cheng, Phys. Rev. B **73**, 012101 (2006).

[13] J. Uddin, V. Barone, and G. E. Scuseria, Mol. Phys. **104**, 745 (2006).

[14] G. A. J. Amaratunga, Science **297**, 1657 (2002).

[15] G. Kresse and D. Joubert, Phys. Rev. B **59**, 1758 (1999), and references therein.

[16] J. P. Perdew and Y. Wang, Phys. Rev. B **45**, 13244 (1992).

[17] D. M. Ceperley and B. J. Alder, Phys. Rev. Lett. **45**, 566 (1980).

[18] J. Paier, M. Marsman, K. Hummer, G. Kresse, I. C. Gerber, and J. G. Ángyán, J. Chem. Phys. **125**, 249901 (2006).

[19] Xing-Qiu Chen, W. Wolf, R. Podloucky, and P. Rogl, Phys. Rev. B **71**, 174101 (2005).

[20] D. Roundy, C. R. Krenn, M. L. Cohen, and J. W. Morris, Jr., Phys. Rev. Lett. **82**, 2713 (1999).

[21] D. Roundy, C. R. Krenn, M. L. Cohen, and J. W. Morris, Jr., Philos. Mag. A **81**, 1725 (2001).

[22] S.-H. Jhi, S. G. Louie, M. L. Cohen, and J. W. Morris, Jr., Phys. Rev. Lett. **87**, 075503 (2001).

[23] *Numerical Data and Functional Relationship in Science and Technology*, edited by K.-H. Helliwege, O. Madelung, M. Schulz, and H. Weiss, Landolt-Börnstein, New Series, Group III, Vols. 17 and 22, pt. a (Springer, New York, 1982).

[24] S. Fahy and S. G. Louie, Phys. Rev. B **36**, 3373 (1987).

[25] F. M. Gao, J. L. He, E. D. Wu, S. M. Liu, D. L. Yu, D. C. Li, S. Y. Zhang, and Y. J. Tian, Phys. Rev. Lett. **91**, 015502 (2003).

[26] J. L. He, D. L. Yu, R. P. Liu, Y. T. Tian, and H. T. Wang, Appl. Phys. Lett. **85**, 5571 (2004).

[27] Y. Zhang, H. Sun, and C. Chen, Phys. Rev. Lett. **93**, 195504 (2004).

[28] D. Roundy and M. L. Cohen, Phys. Rev. B **64**, 212103 (2001).

[29] X. Blase, P. Gillet, A. San Miguel, and P. Melinon, Phys. Rev. Lett. **92**, 215505 (2004).

[30] H. T. McSkimin and P. Andreatch, J. Appl. Phys. **43**, 985 (1972).